

## Transparent, Plastic, Low-Work-Function Poly(3,4-ethylenedioxythiophene) Electrodes

Linda Lindell,<sup>\*,†</sup> Anick Burquel,<sup>‡</sup> Fredrik L. E. Jakobsson,<sup>§</sup> Vincent Lemaux,<sup>‡</sup> Magnus Berggren,<sup>§</sup> Roberto Lazzaroni,<sup>‡</sup> Jérôme Cornil,<sup>‡</sup> William R. Salaneck,<sup>†</sup> and Xavier Crispin<sup>§</sup>

Department of Physics and Measurement Technology, Linköping University, S-581 83 Linköping, Sweden, Service de Chimie des Matériaux Nouveaux, Université de Mons-Hainaut, Place du Parc 20, B-7000 Mons, Belgium, and Department of Science and Technology, Campus Norrköping, Linköping University, S-60174 Norrköping, Sweden

Received May 9, 2006. Revised Manuscript Received June 15, 2006

Novel applications for flexible electronics, e.g., displays and solar cells, require fully flexible, transparent, stable, and low-work-function electrodes that can be manufactured via a low-cost process. Here, we demonstrate that surface chemistry constitutes a route to producing transparent low-work-function plastic electrodes. The work function of the conducting polymer poly(3,4-ethylenedioxythiophene)-tosylate, or PEDOT-Tos, is decreased by submonolayer surface redox reaction with a strong electron donor, tetrakis-(dimethylamino)ethylene (TDAE), allowing it to reach a work function of 3.8 eV. The interface formed between TDAE and PEDOT is investigated in a joint experimental and theoretical study using photoelectron spectroscopy and quantum chemical calculations.

### 1. Introduction

Because of the developments in the area of flexible electronic systems, novel daily life applications are expected to emerge; for instance, electronic newspapers and wearable electronic devices and displays. Many of those forthcoming applications require high-quality and low-cost production. Promising candidates for materials are conducting polymers. One of the best-known  $\pi$ -conjugated polymers is poly(3,4-ethylenedioxythiophene), or PEDOT, also denoted as PEDT. This conducting polymer is employed in device development mainly because of its excellent electrical conductivity upon doping, stability, and electrooptical properties. PEDOT is almost transparent and highly stable in thin oxidized films.<sup>1–5</sup> Prepared using standard oxidative chemical or electrochemical polymerization methods, the positively doped PEDOT films reach high electrical conductivity (about 550 S/cm)<sup>1,6</sup> and display metallic behavior at low temperature.<sup>6–11</sup> Although this conducting polymer is a potential candidate for

transparent plastic electrodes, its insolubility appears to be a major drawback when processing polymer-based devices. The solubility problem can be circumvented by changing the route for the chemical synthesis. First, EDOT can be chemically polymerized in a polystyrenesulfonic acid (PSS) solution to give a PEDOT-PSS water emulsion. Although PEDOT-PSS is a solution for processability, it is characterized by a lower conductivity (10 S/cm).<sup>12–14</sup> Recently, PEDOT-tosylate films with an electrical conductivity exceeding 1000 S/cm have been grown by vapor-phase polymerization,<sup>15</sup> denoted here as VPP-PEDOT-Tos. The polymer layer is grown by exposing a film made of an oxidizing agent (e.g., Fe(III)-tosylate) to a vapor of the EDOT monomer. The chemical composition is seen in Figure 1. In addition to the higher electrical conductivity compared to electrochemically prepared PEDOT-Tos,<sup>16</sup> this synthesis route allows us to coat any substrate (conductors or insulators).

\* Corresponding author. E-mail: linli@ifm.liu.se. Tel: 46-13-282471. Fax: 46-13-137568.

<sup>†</sup> Linköping University.

<sup>‡</sup> Université de Mons-Hainaut.

<sup>§</sup> Linköping University, Campus Norrköping.

- (1) Groenendaal, L. J. F.; Freitag, D.; Pielartzik, H.; Reynolds, J. R. *Adv. Mater.* **2000**, *12*, 481–494.
- (2) Heywang, G.; Jonas, F. *Adv. Mater.* **1992**, *4*, 116–118.
- (3) Dietrich, M.; Heinze, J.; Heywang, G.; Jonas, F. *J. Electroanal. Chem.* **1994**, *369*, 87–92.
- (4) Winter, I.; Reese, C.; Hormes, J.; Heywang, G.; Jonas, F. *Chem. Phys.* **1995**, *194*, 207–213.
- (5) Pei, Q.; Zuccarello, G.; Ahlskog, M.; Inganäs, O. *Polymer* **1994**, *35*, 1347–1351.
- (6) Petterson, L. A. A.; Carlsson, F.; Inganäs, O.; Arwin, H. *Thin Solid Films* **1998**, *313*, 356–361.
- (7) Kiebooms, R.; Aleshin, A.; Hutchison, K.; Wudl, F. *J. Phys. Chem. B* **1997**, *101*, 11037–11039.
- (8) Aleshin, A.; Kiebooms, R.; Menon, R.; Wudl, F.; Heeger, A. J. *Phys. Rev. B* **1997**, *56*, 3659–3663.

- (9) Aleshin, A. N.; Kiebooms, R.; Yu, H.; Levin, M.; Shlimak, I. *Synth. Met.* **1998**, *94*, 157–159.
- (10) Aleshin, A. N.; Kiebooms, R.; Heeger, A. J. *Synth. Met.* **1999**, *101*, 369–370.
- (11) Chang, Y.; Lee, K.; Kiebooms, R.; Heeger, A. J. *Synth. Met.* **1999**, *105*, 203–206.
- (12) Kim, J. Y.; Jung, J. H.; Lee, D. E.; Joo, J. *Synth. Met.* **2002**, *126*, 311–316.
- (13) Jönsson, S. K. M.; Birgersson, J.; Crispin, X.; Greczynski, G.; Osikowicz, W.; Gon, A. W. D. v. d.; Salaneck, W. R.; Fahlman, M. *Synth. Met.* **2003**, *139*, 1–10.
- (14) Crispin, X.; Marciniak, S.; Osikowicz, W.; Zotti, G.; Gon, A. W. D. v. d.; Louwet, F.; Fahlman, M.; Groenendaal, L.; Schryver, F. D.; Salaneck, W. R. *J. Polym. Sci., Part B: Polym. Phys.* **2003**, *41*, 2561–2583.
- (15) Winther-Jensen, B.; West, K. *Macromolecules* **2004**, *37*, 4538–4543.
- (16) Zotti, G.; Zecchin, S.; Schiavon, G.; Louwet, F.; Groenendaal, L.; Crispin, X.; Osikowicz, W.; Salaneck, W.; Fahlman, M. *Macromolecules* **2003**, *36*, 3337–3344.

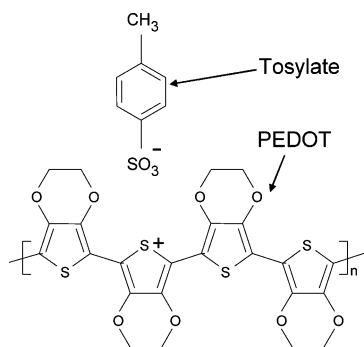


**Figure 1.** Chemical structure of VPP-PEDOT-Tos.

To date, PEDOT-PSS, together with new patterning techniques,<sup>17–19</sup> has been employed in prototype field-effect transistors,<sup>20,21</sup> light-emitting diodes,<sup>22</sup> and photovoltaic cells.<sup>16,23</sup> In the two last devices, PEDOT-PSS was used as a high-work-function (WF = 4.8–5.1 eV) electrode to inject holes into the organic layers, whereas a metal is used when a low-work-function electrode is required to inject electrons. Our motivation is to design low-work-function transparent plastic electrodes to allow electron injection for the next generation of all-plastic flexible solar cells and displays.

At the interfaces in organic devices, the presence of an interface dipole modifies the charge-injection barrier. A simple approach to estimating the electron (hole)-injection barrier at the organic–electrode interface is to consider the energy difference between the electrode work function and the lowest unoccupied molecular orbital, LUMO (highest occupied molecular orbital, HOMO), of the active organic material. An interface dipole with its positive pole pointing toward the organic semiconductor and its negative pole toward the electrode decreases the effective electrode work function. It also lowers the LUMO in the organic layer, with respect to the Fermi energy in the metal, by adding an electrostatic energy. As a result, the electron-injection barrier  $\phi_e$  is reduced, as illustrated in Figure 2. Reversing the interface dipole leads to a reduction in the hole-injection barrier  $\phi_h$ . Thus, a work-function decrease (increase) is associated with an improvement in electron (hole) injection.

Tuning the work function of an electrode surface can be achieved by controlling the orientation of an electric dipole, the interface dipole  $D_{\text{int}}$ . The substrate work-function change,  $\Delta\text{WF}$ , upon monolayer adsorption is a measure of this interface dipole. Although there are various possible origins for the interface dipole potential  $eD_{\text{int}}$ ,<sup>24</sup> it generally consists mainly of the following three contributions:<sup>25,26</sup> First, the reduction of the substrate surface electron density tail upon

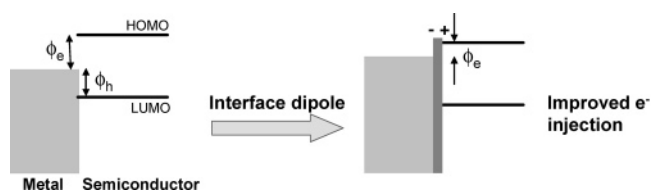


**Figure 2.** Sketch of the impact of the formation of an interface dipole on the electronic levels at an organic semiconductor–metal interface. A traditional simple approach to estimating the electron-injection barrier is to take the difference between the metal work function and the lowest unoccupied molecular orbital (LUMO) of the conjugated material. The electron-injection barrier  $\phi_e$  is modified upon introduction of the interface dipole.

adsorption,<sup>27,28</sup> which always decreases the substrate surface dipole potential  $e\Delta D_{\text{sub}}$ . This contribution can reach up to 1 eV for metal surfaces but is expected to be much smaller for conducting polymer electrodes because of their less-polarizable electronic cloud. Second, the intrinsic dipole moment  $D_{\text{mol}}$  of the adsorbed molecule can tune the work function and charge-injection barrier in devices. For molecules possessing a large dipole moment oriented perpendicular to the metal surface, it has been demonstrated that the total interface dipole could be tuned by chemically changing  $D_{\text{mol}}$ .<sup>29–32</sup> Finally, a chemical dipole potential  $eD_{\text{chem}}$  can be created by partial or total electron transfer between the substrate and the adsorbate upon chemisorption.<sup>33,34</sup> Therefore,  $\Delta\text{WF}$  can be written as a function of these contributions

$$\Delta\text{WF} = eD_{\text{int}} = f(e\Delta D_{\text{sub}}, eD_{\text{mol}}, eD_{\text{chem}}) \quad (1)$$

Recently, we have shown that the chemical dipole potential  $eD_{\text{chem}}$  can be used to significantly tune the electrode work function. Upon chemisorption of a submonolayer of strong electron-donor molecules, the metal and metal-oxide work function could be decreased by 1.5 eV.<sup>35,36</sup> Following our initial studies of the modification of interfacial properties at hybrid interfaces using molecular adsorption, we propose a route to produce low-work-function PEDOT electrodes. The work function of the conducting polymer decreases upon chemisorption of a strong electron-donor molecule, namely tetrakis(dimethylamino)ethylene TDAE [(Me<sub>2</sub>-N)<sub>2</sub>-C=C-(N-Me<sub>2</sub>)<sub>2</sub>] (see Figure 3). TDAE is expected to spontane-

- (17) Service, R. F. *Science* **1997**, *278*, 383–384.  
 (18) Granlund, T.; Nyberg, T.; Stolz Roman, L.; Svensson, M.; Inganäs, O. *Adv. Mater.* **2000**, *12*, 269–273.  
 (19) Stutzmann, N.; Tervoort, T. A.; Broer, D. J.; Siringhaus, H.; Friend, R. H.; Smith, P. *Adv. Funct. Mater.* **2002**, *12*, 105–109.  
 (20) Siringhaus, H.; Kawase, T.; Friend, R. H.; Shimoda, T.; Inbasekaran, M.; Wu, W.; Woo, E. P. *Science* **2000**, *290*, 2123–2126.  
 (21) Lu, J.; Pinto, N. J.; MacDiarmid, A. G. *J. Appl. Phys.* **2002**, *92*, 6033–6038.  
 (22) Kim, W. H.; Mäkinen, A. J.; Nikolov, N.; Shashidhar, R.; Kim, H.; Kafafi, Z. H. *Appl. Phys. Lett.* **2002**, *80*, 3844–3846.  
 (23) Arias, A. C.; Granström, M.; Thomas, D. S.; Petritsch, K.; Friend, R. H. *Phys. Rev. B* **1999**, *60*, 1854–1860.  
 (24) Ishii, H.; Sugiyama, K.; Ito, E.; Seki, K. *Adv. Mater.* **1999**, *11*, 605–625.

- (25) Crispin, X.; Geskin, V. M.; Crispin, A.; Cornil, J.; Lazzaroni, R.; Salaneck, W. R.; Brédas, J. L. *J. Am. Chem. Soc.* **2002**, *124*, 8132–8141.  
 (26) Yan, L.; Watkins, N. J.; Zorba, S.; Gao, Y.; Tang, C. W. *Appl. Phys. Lett.* **2002**, *81*, 2752–2754.  
 (27) Bagus, P. S.; Staemmler, V.; Wöll, C. *Phys. Rev. Lett.* **2002**, *89*, 096104.  
 (28) Lang, N. D. *Phys. Rev. B* **1971**, *4*, 4234–4244.  
 (29) Campbell, I. H.; Kress, J. D.; Martin, R. L.; Smith, D. L.; Barashkov, N. N.; Ferraris, J. P. *Appl. Phys. Lett.* **1997**, *71*, 3528–3530.  
 (30) Zehner, R. W.; Parsons, B. F.; Hsung, R. P.; Sita, L. R. *Langmuir* **1999**, *15*, 1121–1127.  
 (31) Krüger, J.; Bach, U.; Grätzel, M. *Adv. Mater.* **2000**, *12*, 447–451.  
 (32) Vilan, A.; Shanzer, A.; Cahen, D. *Nature* **2000**, *404*, 166–168.  
 (33) Crispin, X.; Lazzaroni, R.; Crispin, A.; Geskin, V. M.; Brédas, J. L.; Salaneck, W. R. *J. Electron Spectrosc. Relat. Phenom.* **2001**, *121*, 57–74.  
 (34) Crispin, X.; Geskin, V.; Lazzaroni, R.; Bureau, C.; Salaneck, W.; Brédas, J. L. *J. Chem. Phys.* **1999**, *111*, 3237–3251.  
 (35) Osikowicz, W.; Crispin, X.; Tengstedt, C.; Lindell, L.; Kugler, T.; Salaneck, W. R. *Appl. Phys. Lett.* **2004**, *85*, 1616–1618.  
 (36) Lindell, L.; Jong, M. P. d.; Osikowicz, W.; Lazzaroni, R.; Berggren, M.; Salaneck, W. R.; Crispin, X. *J. Chem. Phys.* **2005**, *122*, 084712.

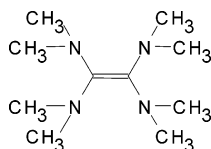


Figure 3. Chemical structure of TDAE.

ously transfer electrons to PEDOT, thus creating a chemical dipole  $D_{\text{chem}}$  that lowers the work function of PEDOT. The interface formed between TDAE and PEDOT is investigated in a joint experimental and theoretical study using photoelectron spectroscopy and quantum chemical calculations. A similar charge transfer and work function decrease are expected with alkali metal deposition on PEDOT. However, the deposition of alkali metal requires sublimation of the reactive metal in a vacuum chamber. In contrast, a much simpler process can be used for TDAE. Indeed, the vapor pressure at room temperature of the liquid TDAE in a nitrogen atmosphere is enough to induce the surface modification of PEDOT. Moreover, alkali metal atoms are expected to diffuse through the polymer layer, whereas the bulky TDAE molecules cannot penetrate in the VPP-PEDOT-Tos films.

## 2. Experimental Details

**2.1. Synthesis of the VPP-PEDOT-Tos.** The vapor-phase polymerized PEDOT samples are fabricated using a procedure similar to that described by Winther-Jensen et al.<sup>15,37</sup> The substrates are washed in a mixture of DI water, HNO<sub>3</sub>, and H<sub>2</sub>O<sub>2</sub> (5:1:1) at 80 °C for 10 min, followed by careful rinsing with DI water. A solution of 40 wt % ferric *p*-toluenesulfonate (Fe(III) tosylate) and 2.8 wt % pyridine in butanol is spin-coated onto the glass substrates. The samples are thereafter transferred into a polymerization chamber and exposed to a vapor of 3,4-ethylenedioxythiophene (EDOT) at 50 °C for 30 min. After the polymerization process, the excess Fe(III) tosylate is removed by washing the surfaces with ethanol.

**2.2. Photoelectron Spectroscopy.** Measurements are performed using an ESCA 200 spectrometer. The spectrometer is equipped with a monochromatized Al(K<sub>α</sub>) X-ray source ( $h\nu = 1486.6$  eV) with a base pressure of  $1 \times 10^{-10}$  mbar. The energy resolution obtained with the chosen experimental conditions is such that the full width at half-maximum (fwhm) of the gold (Au(4f<sub>7/2</sub>)) line is 0.65 eV. The UPS spectra are obtained using a He resonance lamp for HeI radiation ( $h\nu = 21.2$  eV) with a resolution of 0.1 eV determined from the width of the Fermi edge of a gold substrate. PEDOT films are vapor-phase polymerized on both polycrystalline gold and glass substrates. There are no significant differences in quality of the VPP-PEDOT-Tos films, depending on substrate. Thereafter, the polymer film is introduced in the spectrometer for in situ exposure to a vapor of TDAE. The liquid TDAE is kept in a glass container and connected to the preparation chamber of the spectrometer via a separate gas handling system. The deposition of TDAE monolayers is made at room temperature, i.e., well above its condensation temperature ( $T_{\text{condensation}} \approx -70$  °C at  $p_{\text{background}} = 1 \times 10^{-10}$  mbar) to prevent multilayer formation. The pressure in the preparation chamber is measured to be in the range  $5 \times 10^{-9}$  to  $2 \times 10^{-8}$  mbar during evaporation of TDAE. When the monolayers, or possibly submonolayers, are formed on VPP-PEDOT-Tos, the TDAE exposure continues until saturation is

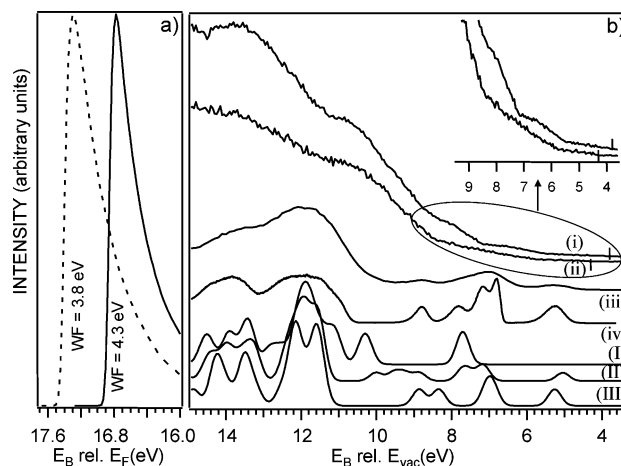


Figure 4. (a) Electron cutoff of the UPS He(I) spectra of VPP-PEDOT-Tos before (full line) and after (dashed line) deposition of TDAE monolayer at room temperature. Binding energies, in eV, are relative to the Fermi level. (b) Valence levels spectra of (i) TDAE monolayer on VPP-PEDOT-Tos, (ii) VPP-PEDOT-Tos, (iii) TDAE multilayer, and (iv) TDAE in the gas phase. The theoretical UPS spectra for (I) doubly charged, (II) singly charged, and (III) neutral TDAE are also included. Binding energies, in eV, are relative to the vacuum level. The vertical lines in the inset indicate the position of the Fermi level of the spectrometer. The calculated data of the right panel are adapted from W. Osikowicz et al.<sup>35</sup>

achieved according to UPS and XPS signals. Multilayer TDAE films are formed by condensing a molecular vapor on the cold substrates ( $T \approx -100$  °C). The resulting multilayer film shows no trace of O(1s) contamination. The photoelectrons are collected normal to the surface or, when specified as grazing angle, at 60° with respect to the surface normal. The binding energies are measured relative to the Fermi level of the spectrometer. The work function of the surface is obtained as the difference between the secondary electron cutoff in the UPS spectrum and the photon energy used.<sup>38</sup>

## 3. Experimental Results

**3.1. Work Function Modification.** TDAE is known as a potent reductant,<sup>39</sup> which adopts either of two oxidation states, TDAE<sup>+</sup> or TDAE<sup>2+</sup>.<sup>40,41</sup> The oxidation potential of TDAE is almost comparable to that of zinc,<sup>42</sup> which can reduce the positively doped PEDOT. Hence, TDAE is expected to transfer an electron to VPP-PEDOT-Tos. The UPS secondary electron cutoff (Figure 4a) displays a decrease in the VPP-PEDOT-Tos work function from  $4.3 \pm 0.05$  eV to  $3.8 \pm 0.05$  eV upon in situ exposure of TDAE at room temperature. The modification in work function is the first indication that the surface is modified by chemisorption of a submonolayer of TDAE. Note that the modified surface has a work function lower than that of an aluminum(-oxide) electrode (4.1 eV) known as a reason-

(37) Winther-Jensen, B.; Breiby, D. W.; West, K. *Synth. Met.* **2005**, *152*, 1–4.

(38) Salaneck, W. R.; Stafström, S.; Brédas, J. L. *Conjugated Polymer Surfaces and Interfaces: Electronic and Chemical Structure of Interfaces for Polymer Light Emitting Devices*; Cambridge University Press: Cambridge, U.K., 1996.

(39) Kuroboshi, M.; Tanaka, M.; Kishimoto, S.; Goto, K.; Mochizuki, M.; Tanaka, H. *Tetrahedron Lett.* **2000**, *41*, 81–84.

(40) Allemand, P.-M.; Khemani, K. C.; Koch, A.; Wudl, F.; Holczer, K.; Donovan, S.; Gruner, G.; Thompson, J. D. *Science* **1991**, *253*, 301–303.

(41) Fox, J. R.; Foxman, B. M.; Guarrera, D.; Miller, J. S.; Calabrese, J. C.; Reis, A. H. *J. Mater.* **1996**, *6*, 1627–1631.

(42) Burkholder, C.; Dolbier, W. R.; Médebielle, M. *J. Org. Chem.* **1998**, *63*, 5385–5394.

able electron-injecting electrode in polymer light-emitting diodes. The shift in work function (0.5 eV) is attributed to the formation of a surface dipole due to electrons transferred from TDAE molecules to VPP-PEDOT-Tos, thus creating a surface chemical dipole  $D_{\text{chem}}$ . In the following investigation, we aim at understanding this surface chemical reaction.

**3.2. Analysis of the Valence Electronic Levels.** Figure 4b displays the UPS spectra of the valence electronic levels of (i) the TDAE-modified VPP-PEDOT-Tos surface, (ii) VPP-PEDOT-Tos, (iii) a TDAE multilayer, and (iv) TDAE in the gas phase. The theoretical UPS spectra for (I) doubly charged, (II) singly charged, and (III) neutral TDAE are also included in this figure. The general procedure used to calculate the UPS spectra has been described in detail elsewhere.<sup>43</sup> Briefly, we simulate the spectra within Koopmans' approximation (i.e., using the absolute value of the eigenvalues as binding energies), without estimating cross-sections and by matching the HOMO of the single molecule to the ionization potential in the UPS spectrum (vs vacuum level) obtained for the TDAE multilayer in order to account for solid-state polarization effects. The energy scale of the DFT-B3LYP eigenvalues has been contracted by a factor of 0.95 to compensate for the neglect of intramolecular electronic relaxation and correlation effects. The broadening of the UPS features is introduced with the help of Gaussian functions (with a full width at half-maximum set at 0.4 eV if not otherwise stated) centered on each eigenvalue. For singly and doubly charged TDAE molecules, the eigenvalue spectra have been shifted in order to have similar sigma levels (at binding energies higher than 8 eV) compared to the neutral TDAE. From the experimental UPS spectra (solid phase), the ionization potential (IP) associated with the HOMO of TDAE is 5.2 eV vs vacuum level. The gas phase and theoretical UPS spectra, after adjusting the energy scale, reproduce well the shape of the UPS spectrum for the multilayer.

Before TDAE exposure, VPP-PEDOT-Tos is positively doped and a broad and flat distribution of (bi)polaronic levels from the PEDOT chain are visible in the energy range from approximately 6 to 4 eV with energy referred to the vacuum level<sup>44</sup> (see spectrum (ii) in Figure 4b). When analyzing the changes in the UPS spectrum of VPP-PEDOT-Tos after deposition of a TDAE monolayer, the most important observation is that there is no additional feature appearing in the monolayer spectrum in the energy region around 5 eV. Compared with the theoretical valence levels of TDAE, TDAE<sup>+</sup>, and TDAE<sup>2+</sup>, the absence of a new signal in this region indicates that no neutral TDAE molecules or cationic TDAE<sup>+</sup> are present at the VPP-PEDOT-Tos surface. Indeed, those species would display a signal corresponding to the HOMO level (doubly occupied for TDAE and singly occupied for TDAE<sup>+</sup>). This suggests that two electrons are transferred from TDAE to the VPP-PEDOT-Tos surface. The

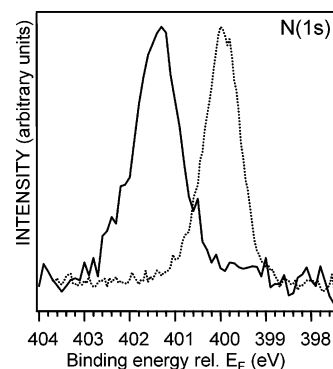


**Figure 5.** N(1s) XPS spectra of a TDAE multilayer (dotted line) and the TDAE monolayer deposited on VPP-PEDOT-Tos (full line). Binding energies are referred to the Fermi level.

probing depth of the UPS He(I) is about 10–15 Å,<sup>45</sup> and because the polymer surface is modified with only a (sub)-monolayer, valence electrons in the VPP-PEDOT-Tos surface still contribute significantly to the photoemission signal after TDAE deposition. The new signal appearing at 6.5 eV, which cannot be explained from the electronic structure of either TDAE<sup>+</sup>, TDAE<sup>2+</sup>, or TDAE, may possibly be attributed to the HOMO of neutral PEDOT segments created by dedoping the positively doped VPP-PEDOT chains. The IP of neutral phenyl-capped EDOT oligomers, which are a model system for a neutral PEDOT chain, corresponds typically to that binding energy.<sup>46,47</sup> The contribution appearing at 7.7 eV might come from the HOMO level of TDAE<sup>2+</sup> (related to the shape of the HOMO-1 for neutral TDAE).

**3.3. Core-Level Analysis.** The surface reaction has been followed by tracking the N(1s) core level of TDAE. A first observation is that TDAE adsorbs on the surface at room temperature. A second observation is that upon longer exposure to TDAE, the TDAE amount does not increase on the surface, thus indicating that TDAE does not condense or diffuse into the dense polymer film. The N(1s) spectrum of a neutral TDAE multilayer is characterized by a single peak located at 400.0 eV relative to  $E_F$  (Figure 5), which supports the neutral TDAE molecules having four chemically equivalent nitrogen atoms. The TDAE monolayer chemisorbed on VPP-PEDOT-Tos is characterized by an N(1s) peak shifted 1.4 eV toward higher binding energy relative to the multilayer peak. The single N(1s) peak, although slightly broadened, confirms that the four nitrogen atoms in the chemisorbed TDAE molecule are chemically equivalent and that all TDAE molecules present at the surface undergo the same reaction. The minor broadening of the peak is likely due to the presence of VPP-PEDOT-Tos that screens the core hole differently. The significant core-level shift indicates that the nitrogen atoms lose part of their electronic density; in other words, that TDAE is positively charged in the chemisorbed monolayer. Calculations of differently charged states of TDAE<sup>48</sup> show that doubly charged TDAE<sup>2+</sup> has

(43) Cornil, J.; Vanderdonck, S.; Lazzaroni, R.; Santos, D. A. d.; Thys, G.; Geise, H. J.; Yu, L.-M.; Szablewski, M.; Bloor, D.; Lögdlund, M.; Salaneck, W. R.; Gruhn, N. E.; Lichtenberger, D. L.; Lee, P. A.; Armstrong, N. R.; Brédas, J. L. *Chem. Mater.* **1999**, *11*, 2436–2443.  
 (44) Greczynski, G.; Kugler, T.; Keil, M.; Osikowicz, W.; Fahlman, M.; Salaneck, W. R. *J. Electron Spectrosc. Relat. Phenom.* **2001**, *121*, 1–17.

(45) Nielsen, P.; Sandman, D. J.; Epstein, A. J. *Solid State Commun.* **1975**, *17*, 1067–1071.

(46) Osikowicz, W.; Gon, A. W. D. v. d.; Crispin, X.; Jong, M. d.; Friedlein, R.; Groenendaal, L.; Fahlman, M.; Beljonne, D.; Lazzaroni, R.; Salaneck, W. R. *J. Chem. Phys.* **2003**, *119*, 10415–10420.

(47) Jong, M. P. d.; Gon, A. W. D. v. d.; Crispin, X.; Osikowicz, W.; Salaneck, W. R.; Groenendaal, L. *J. Chem. Phys.* **2003**, *118*, 6495–6502.

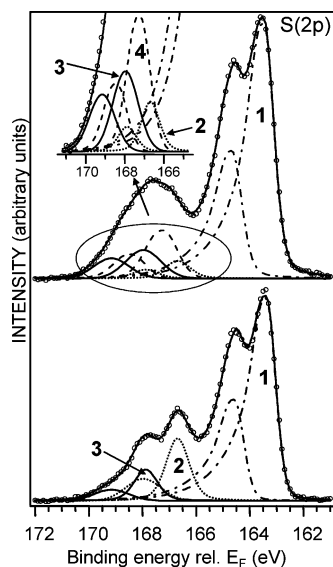


**Figure 6.** S(2p) XPS spectra of the VPP-PEDOT-Tos surface (below) and the same surface after TDAE monolayer deposition (above). Binding energies are referred to Fermi level.

the positive charge localized along the N–C–N bonds and thus gives rise to one N(1s) XPS peak only. In the case of singly positive charged TDAE, there are two possible configurations found in the potential energy surface, one with a symmetric charge distribution that would give rise to one XPS N(1s) peak and one with an asymmetric unpaired energy density distribution that would give rise to two XPS N(1s) peaks. The latter arrangement is not likely to occur in this case, because only one peak is observed.

For chemisorbed molecules present in the electrostatic potential drop at the surface, the choice of a reference energy level is a common problem.<sup>49</sup> The energy shift of the N(1s) signal depends on the energy reference used for the binding energy axis. Using the Fermi level as reference, the energy shift is 1.4 eV, whereas it is as large as 2.1 eV relative to the vacuum level. The N(1s) binding energies of many compounds (amines, nitrile, etc.) are often found relatively close to each other. In contrast, the N(1s) signal of compounds with functional groups such as  $(\text{NH}_3)^+\text{Cl}^-$  or  $(\text{N}(\text{CH}_3)_3)^+\text{Cl}^-$  is shifted toward higher binding energies by 1.5–2.1 eV.<sup>50</sup> Hence, considering a shift of at least 1.4 eV for the N(1s) peak of TDAE, the XPS results supported by the UPS data indicate that TDAE molecules present on the polymer surface carry two positive charges.

The XPS spectrum for the S(2p) photoelectrons allows us to distinguish between PEDOT and tosylate anions. Using shape-splitting between S(2p) doublets and binding energies of peaks from previously made data analysis of PEDOT derivatives,<sup>16</sup> it can be concluded that the S(2p) signal from VPP-PEDOT-Tos consists of at least three doublets (see bottom spectrum in Figure 6). The main doublet at 163.4 eV (peak 1) is attributed to the sulfur atoms in the PEDOT chains, whereas the two doublets visible at higher binding

energies originate from negatively charged tosylate molecules acting as charge balancing counterions to the positively doped PEDOT (peak 2 at 166.7 eV), along with two Fe(II) tosylate cations remaining after the oxidative EDOT polymerization (peak 3 at 168.0 eV). The doping level of VPP-PEDOT-Tos, extracted from the relative intensity of the S(2p) signals from PEDOT and its counterion tosylate, is about 0.22–0.25 positive charge per EDOT units. From the Fe(2p) core level, it is concluded that the remaining iron is the dication originating from the reduction of  $\text{Fe}(\text{III})(\text{Tos})_3$  after the reaction with EDOT during the polymerization. The surface of the films contains about one  $\text{Fe}(\text{II})(\text{Tos})_2$  every nine EDOT units.

As the VPP-PEDOT-Tos surface is exposed to TDAE, the shape of the S(2p) signal belonging to the tosylate anions is modified (see the top spectrum in Figure 6). This can be explained only if a new doublet is introduced at 167.3 eV (peak 4) in the deconvolution of the spectrum. The Fe(2p) peak is not shifted or changed upon TDAE deposition, which indicates that the  $\text{Fe}(\text{II})(\text{Tos})_2$  is not further reduced by TDAE. Consequently, the relative intensity between the PEDOT signal and the  $\text{Fe}(\text{II})(\text{Tos})_2$  is kept constant as well as the shape and binding energy in the peak-fitting analysis. The new doublet is located between the two representing Fe(II) tosylate and negatively charged tosylate ions. The growth of the new features is accompanied by a significant decrease in intensity of the doublet associated to the tosylate cations that balance the positively doped PEDOT chains. This observation is consistent with the electron transfer from the TDAE to the positively doped chains. Indeed, this undoping process is accompanied by the release of the tosylate cation from the PEDOT chains and their attraction to the newly formed, positively charged TDAE molecules. The O(1s) spectrum (not shown here) indicates also that tosylate anions change orientation and/or position upon TDAE exposure. The rearrangement of tosylate might be an explanation for the relatively low work-function change compared to the large local dipole created by a two-electron-transfer reaction between TDAE and PEDOT.

#### 4. Theoretical Models and Results

Quantum-chemical calculations have been performed to characterize the electron-transfer reactions from a TDAE molecule (acting as the donor, D) to a PEDOT segment supporting a bipolaron (acting as the acceptor, A). To get a deeper insight into the interfacial interactions, we have built a model system initially incorporating (see Figure 7) (i) a doubly charged PEDOT oligomer containing six repeat units in a planar conformation (this size is representative of the typical extent of a bipolaron in conjugated polymer chains);<sup>51</sup> (ii) two singly negatively charged counterions lying in the plane of the conjugated chain, each represented by a sparkle in the calculations (i.e., an unpolarizable ion with a diameter of 1.4 Å, introducing only an electrostatic perturbation); and (iii) a neutral TDAE molecule located on top of the center of the PEDOT chain, with a distance of 3.5 Å between the

(48) Pokhodnia, K. I.; Papavassiliou, J.; Umek, P.; Omerzu, A.; Mihailovic, D. *J. Chem. Phys.* **1999**, *110*, 3606–3611.

(49) W. F. Egelhoff, J. *Surf. Sci. Rep.* **1987**, *6*, 253–415.

(50) Beamson, G.; Briggs, D. *High Resolution XPS of Organic Polymers: The Scienta ESCA300 Database*; John Wiley & Sons Ltd.: New York, 1992.

(51) Cornil, J.; Beljonne, D.; Brédas, J. L. *J. Chem. Phys.* **1995**, *103*, 842–849.

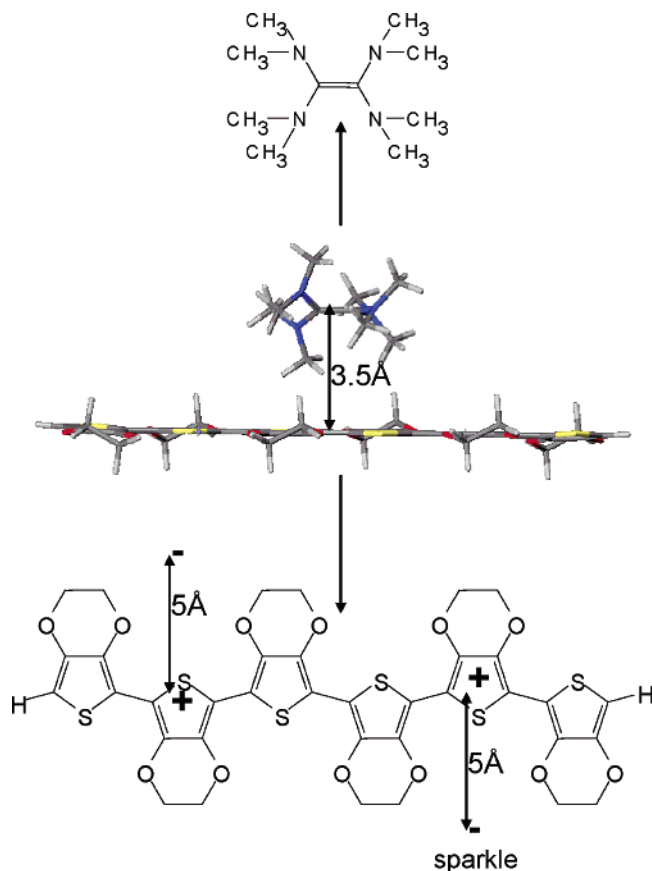


**Figure 7.** Chemical structure of the model complex composed of an EDOT oligomer and a TDAE molecule.

plane of the chain and the central C–C double bond of the TDAE molecule. The choice of the planar conformation for the PEDOT oligomer is validated by the fact that doping leads to the appearance of a quinoid character within the thiophene rings, thus preventing significant torsions of the conjugated backbone.<sup>51</sup>

On that basis, the change in the total energy of the initial complex when transferring one or two charges from the TDAE molecule to the PEDOT chain is calculated. This energy difference has to be negative for the electron transfer to be thermodynamically favorable (the entropic contributions are neglected here). In the case of a single charge transfer, we thus calculate

$$\Delta E = E(D^+A^-) - E(DA) = [E(\text{TDAE}^{1+}) + E(\text{PEDOT}^{1-})] - [E(\text{TDAE}) + E(\text{PEDOT})] + \Delta E_{\text{coul}}$$

where  $E(\text{TDAE})$  and  $E(\text{TDAE}^{1+})$  are the total energies of TDAE in the ground state and singly charged state, respectively, whereas  $E(\text{PEDOT})$  and  $E(\text{PEDOT}^{1-})$  are the energies of the PEDOT oligomer in the pristine state (with two positive charges and two associated counterions) and the singly charged state (one positive charge and two counterions), respectively.  $\Delta E_{\text{coul}}$  accounts for the change in the Coulomb attraction between the TDAE molecule and the PEDOT chain together with its two counterions during the transfer; this is a stabilization term driven by the appearance of a dipole across the donor–acceptor interface upon charge transfer. Similar expressions are used when two charges are

transferred from TDAE to PEDOT. To evaluate those energies, we optimized the structure of the PEDOT chain in the three redox states, in the presence of the counterions and by imposing the planarity of the conjugated backbone, with the help of the semiempirical Hartree–Fock Austin Model 1 (AM1) method<sup>52</sup> coupled to a full configuration interaction (FCI) scheme within a limited active space, as implemented in the Ampac package.<sup>53</sup> The number of orbitals is chosen to ensure the convergence of the calculated energies. The total energy of the PEDOT chain is then estimated from the generated structure by coupling the AM1-FCI formalism to the COSMO model<sup>54</sup> in order to take into account the polarization effects in the surrounding dielectric medium that stabilize the system; this medium is here assumed to be isotropic and characterized by a static dielectric constant,  $\epsilon_s$ , of 3. The structures of neutral, singly, and doubly charged TDAE have been fully optimized at the density functional theory (DFT) level, using the hybrid Becke–Lee–Yang–Parr (B3LYP) functional and a standard 6-31G\*\* basis set. Those optimized structures have been validated previously.<sup>35</sup> The corresponding total energies have been estimated at the AM1-FCI/COSMO level for the sake of coherence. The Coulomb attraction term has been estimated by summing by pairs all interactions between the atomic charges on the donor (TDAE) and the acceptor (PEDOT + counterions). For a single charge transfer

$$\Delta E_{\text{coul}} = \sum_{D^+} \sum_{A^-} \frac{q_D q_{A^-}}{4\pi\epsilon_0\epsilon_s r_{D+A^-}} - \sum_D \sum_A \frac{q_D q_A}{4\pi\epsilon_0\epsilon_s r_{DA}}$$

$q_D$  and  $q_A$  correspond to the atomic charges on the donor and acceptor in their relevant states; they have been obtained from a population analysis performed within the ZDO (zero differential overlap) approximation from the AM1-CI/COSMO results. We stress that this approach has been shown to provide  $\Delta E$  values for electron-transfer reactions in good agreement with corresponding experimental data for model donor/acceptor complexes.<sup>55</sup>

Using the scheme above, the adsorption energy can be estimated by  $\Delta E$  that is equal to  $-1.1$  eV when transferring one charge from TDAE to PEDOT for an intermolecular distance of  $3.5$  Å. A  $\Delta E$  value of  $+1.5$  eV is obtained when replacing TDAE by an ethylene molecule; this demonstrates that the strong donor character of TDAE is a prerequisite for rendering the charge transfer thermodynamically favorable. Interestingly,  $\Delta E$  further increases down to  $-1.5$  eV with respect to the initial state for a double charge transfer between the donor and the acceptor. This evolution is driven by the Coulomb attraction term ( $-2.5$  eV), which compensates for the energy required to generate separately the doubly charged TDAE molecule and the neutral PEDOT chain surrounded by two negative counterions ( $+1.0$  eV). Figure 8a illustrates that the  $\Delta E$  value associated with a single

(52) Dewar, M. J. S.; Zoebisch, E. G.; Healy, E. F.; Stewart, J. J. P. *J. Am. Chem. Soc.* **1985**, *107*, 3902–3909.

(53) AMPAC, version 6.55; Semiche, Inc.: Shawnee Mission, KS, 1997.

(54) Klamt, A.; Schürmann, G. *J. Chem. Soc., Perkin Trans.* **1993**, *2*, 799–805.

(55) Pourtois, G.; Beljonne, D.; Cornil, J.; Ratner, M. A.; Bredas, J. L. *J. Am. Chem. Soc.* **2002**, *124*, 4436–4447.

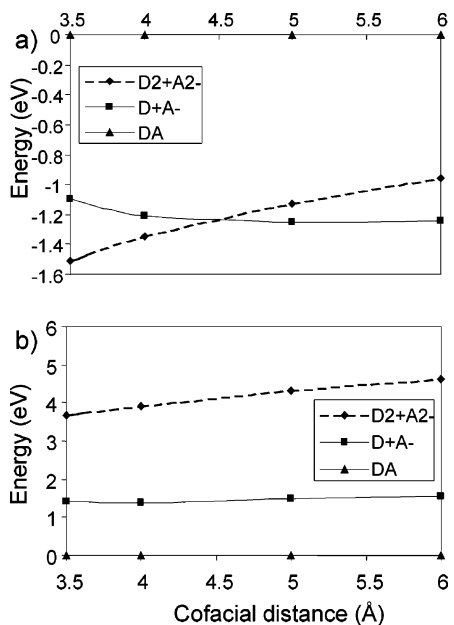


**Figure 8.** Evolution of  $\Delta E$ , an estimate of the adsorption energy, for the complex in the three different states as a function of the intermolecular distance.

charge-transfer remains almost constant when increasing the intermolecular distance from 3.5 to 6 Å. The energy gained by transferring two electrons is reduced by 0.5 eV going from 3.5 to 6 Å but is kept in the negative range, thus implying that the occurrence of a double charge transfer is not affected by changes in the intermolecular distances at the interface. Interestingly, the same curves generated in the absence of the counterions yield positive and large values for  $\Delta E$  (see Figure 8b). This indicates that the charge transfer cannot occur in the presence of neutral PEDOT chains.

The impact of the rotational disorder on the electron-transfer process is investigated by looking at the evolution of  $\Delta E$  when rotating TDAE on top of the center of the PEDOT chain (see Figure 9). The  $\Delta E$  values are found to be slightly affected by these geometric fluctuations; because similar observations prevail when translating TDAE along the PEDOT chain, we are led to the conclusion that the efficiency of the charge transfer is not strongly tributary of the exact interfacial geometry between the donor and acceptor units.

## 5. Conclusions

The surface of a conducting VPP-PEDOT-Tos electrode ( $\sigma \approx 1000$  S/cm) is modified by surface redox reaction with a strong electron donor, TDAE. This surface modification allows for the creation of a transparent, low-work-function, plastic electrode. The work function reaches 3.8 eV, which is lower than that of the aluminum-(oxide) electrode (4.1 eV) known as a reasonable electron-injecting electrode in polymer light-emitting diodes.

Results from theoretical calculations as well as the UPS and XPS measurements indicate that electrons are transferred

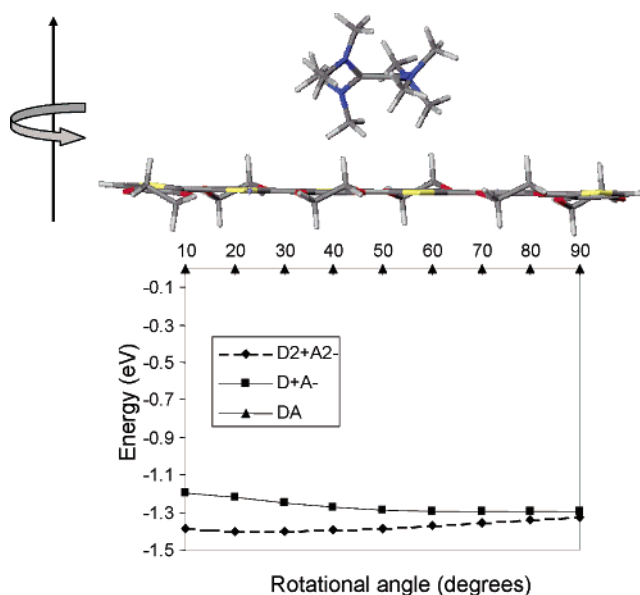


**Figure 9.** Evolution of  $\Delta E$ , an estimate of the adsorption energy, for the complex in the three different states as a function of the rotational angle of the TDAE molecule on top of the PEDOT chain. The intermolecular distance is fixed here at 4 Å.

from TDAE to the VPP-PEDOT-Tos surface, which creates a surface dipole that lowers the work function by 0.5 eV. The UPS data show that neutral EDOT oligomers are created upon TDAE exposure because of the undoping of some segments of the pristine, positively doped PEDOT chains. The N(1s) XPS spectra indicate that TDAE is doubly positively charged when adsorbed on VPP-PEDOT-Tos. The driving force of the TDAE chemisorption on the polymer surface is the electrostatic attraction between tosylate in the polymer film and TDAE<sup>2+</sup> formed after electron transfer to the PEDOT chains. The theoretical calculations support the occurrence of a double charge transfer from each TDAE molecule, as inferred by the photoelectron spectroscopy results. We believe that surface redox reaction can be used to modify the work function of many surfaces, including conducting polymer surfaces. This is a simple route for controlling the work function of electrodes in organic electronic devices.

**Acknowledgment.** The authors gratefully acknowledge The Swedish Foundation for Strategic Research (COE@COIN), VINNOVA, The Royal Swedish Academy of Sciences, and The Swedish Research Council for financial support of this project. The Mons–Linköping collaboration is within the EU Integrated Project NAIMO (NMP4-CT-2004-500355). The work in Mons has been supported by the Belgian Federal Government “Interuniversity Attraction Pole in Supramolecular Chemistry and Catalysis, PAI 5/3” and the Belgian National Fund for Scientific Research (FNRS/FRFC). J.C. is an FNRS Research Associate. In addition, the authors thank Olle Inganäs, Emilien Saindon, and Wojciech Osikowicz for stimulating discussions.